

A Proton-Induced N-1 to η^2 Migration of the Fluxional Pyrazine in the $[\text{Ru}^{\text{II}}(\text{hedta})(\text{pz})]^-$ Complex

Ya Chen and Rex E. Shepherd*

Department of Chemistry, University of Pittsburgh, Pittsburgh, Pennsylvania 15260

Received October 18, 1996

$[\text{Ru}^{\text{II}}(\text{hedta})(\text{D}_2\text{O})]^-$, $\text{hedta}^{3-} = N$ -(hydroxyethyl)ethylenediaminetriacetate, reacts with pyrazine in D_2O at 25 °C to yield several isomers and $\leq 20\%$ of the pyrazine-bridged binuclear complex. Two isomers of 56.2% combined abundance have differentiated α (near) and β (remote) ^1H NMR pyrazine resonances at 9.09 ppm (α or H2, H6 pair) and 8.33 ppm (β or H3, H5 pair). The other isomer of ca. 24% abundance exhibits only a singlet at 8.76 ppm, indicative of fluxional pyrazine movement from N-1 to N-4. This is believed to be the cis-polar isomer. Within 24 h the differentiated isomers convert to the fluxional isomer, which remains fluxional in 50% $\text{D}_2\text{O}/50\%$ CD_3OD down to 237 K. The fluxional isomer has all equivalent ^{13}C NMR resonances at 152.44 ppm, 5.18 ppm downfield of free pyrazine. Comparison with the bridged binuclear ion $\{[\text{Ru}(\text{hedta})]_2(\text{pz})\}^{2-}$ revealed fortuitously similar shifts; the ^1H NMR spectrum shows a singlet at 8.76 ppm, and the ^{13}C NMR spectrum, a singlet at 152.40 ppm. These species have different electrochemical signatures, however, with the 1:1 fluxional complex having a $\text{Ru}^{\text{II/III}}$ wave at 0.20 V that shifts to 0.35 V upon protonation of the N-4 position, whereas the binuclear complex has two waves at 0.18 and 0.33 V which are independent of pH. ^1H NMR indicates stereochemically rigid coordination of 2-methylpyrazine (2- CH_3pz) at N-4 with the 2- CH_3 position remote in the major species (65.5%) and at N-2 with the 2- CH_3 site adjacent (34.4%) in the lesser isomer. The proton resonances are as follows. Remote isomer (N-4): H2, 8.22 ppm; H3, 8.97 ppm; H5, 8.88 ppm; CH_3 , 2.53 ppm. Adjacent (N-1) isomer: H2, 8.73 ppm; H3, 8.42 ppm, H5, 8.50 ppm; CH_3 , 2.45 ppm. A slow conversion of the strained adjacent isomer to the remote isomer is observed. Remote and adjacent isomers were also prepared for $[(\text{NH}_3)_5\text{Ru}(2\text{-CH}_3\text{pz})]^{2+}$ in 87.7% and 12.3% yield. Protonation of $[\text{Ru}(\text{hedta})(\text{pz})]^-$ yields nonfluxional complexes: a major species (63%) bound $\eta^2(1,2)$ with four complicated resonance patterns at 8.72, 8.57, 8.00, and 7.91 ppm, each signal having across-the-ring couplings which require couplings to at least two different ring protons and a minor N-1-coordinated N-4 protonated species (16%) with α and β proton pairs resonating at 8.81 and 8.25 ppm. An η^2 -(2,3) isomer is also detectable (20%) which has four types of ^1H resonances at 9.51, 9.01, 8.85, and 8.15 ppm. The weakened σ bonding from pzH^+ and enhanced π -acceptor capacity power of pzH^+ combine to induce a switch in coordination to either $\eta^2(1,2)$ or $\eta^2(2,3)$.

Introduction

The pyrazine ligand has had a special influence on the development of concepts of π -back-bonding between Ru^{II} centers and N-heterocyclic rings.^{1–9} Pyrazine and methylated pyrazines have been used as pH-dependent probes to assess the degree of π -back-donation by Ru^{II} ,^{1,8} and as an indirect monitor of the influence of other spectator ligands such as CN^- and polyaminopolycarboxylate ligands in modifying Ru^{II} 's capacity to π -donate.^{6–9} Numerous mixed-valence complexes involving pyrazine ligand bridges have been studied in order to examine changes in metal–metal center couplings through pyrazine

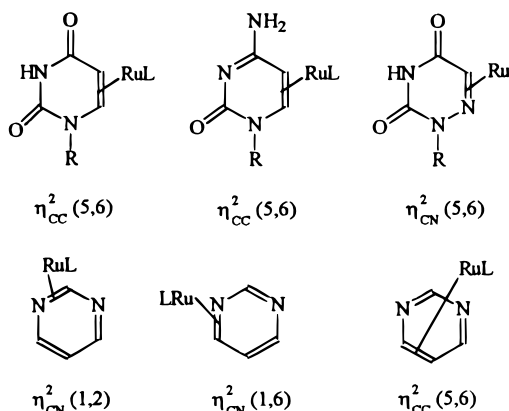
bridges, stimulated by observations for the original Creutz–Taube ion.^{2–5}

In none of these studies of Ru^{II} complexes with pyrazines has there been mention of coordination of the various pyrazine ligands in any mode other than attachment at the N-1 lone pair of electrons. The η^2 attachment of ruthenium(II) polyamino polycarboxylates, particularly $[\text{Ru}^{\text{II}}(\text{hedta})]^-$, has been recently established for uracils and uridines,^{10–12} cytosine and cytidines,¹⁰ the RNA polymerase inhibitor 6-azauridine,¹³ and simple pyrimidines and methylpyrimidines.^{14–16} Factors affecting the change from N-1 to η^2 -attachment are discussed in earlier publications.^{10–16} Representative structures of these η^2 com-

- (1) Ford, P.; Rudd, D. P.; Gaunders, R. G.; Taube, H. *J. Am. Chem. Soc.* **1968**, *90*, 1187.
- (2) (a) Creutz, C.; Taube, H. *J. Am. Chem. Soc.* **1973**, *95*, 1086. (b) Creutz, C.; Taube, H. *J. Am. Chem. Soc.* **1969**, *91*, 3988.
- (3) (a) Citrin, P. H.; Ginsberg, A. P. *J. Am. Chem. Soc.* **1981**, *103*, 3673. (b) Meyer, T. J. *Prog. Inorg. Chem.* **1983**, *30*, 389.
- (4) (a) Creutz, C. *Prog. Inorg. Chem.* **1983**, *30*, 1. (b) Wong, K.; Schatz, P. N. *Prog. Inorg. Chem.* **1981**, *28*, 370.
- (5) (a) McClendon, G. *Coord. Chem. Rev.* **1985**, *68*, 1. (b) Richardson, D. E.; Taube, H. *Coord. Chem. Rev.* **1984**, *60*, 107. (c) Sneddon, K. R. *Coord. Chem. Rev.* **1982**, *41*, 29.
- (6) Johnson, C. R.; Shepherd, R. E. *Inorg. Chem.* **1983**, *22*, 1117.
- (7) Henderson, W. W.; Shepherd, R. E. *Inorg. Chem.* **1985**, *24*, 2398.
- (8) Toma, H. E.; Stadler, E. *Inorg. Chem.* **1985**, *24*, 3085.
- (9) Zhang, S.; Shepherd, R. E. *Transition Met. Chem.* **1992**, *17*, 199.

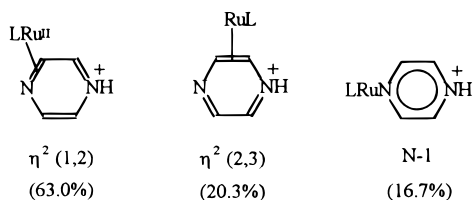
- (10) Zhang, S.; Holl, L. A.; Shepherd, R. E. *Inorg. Chem.* **1990**, *29*, 1012.
- (11) Shepherd, R. E.; Zhang, S.; Lin, F.-T.; Kortes, R. A. *Inorg. Chem.* **1992**, *31*, 1457.
- (12) Zhang, S.; Shepherd, R. E. *Inorg. Chim. Acta* **1992**, *191*, 271.
- (13) Chen, Y.; Shepherd, R. E. *Inorg. Chim. Acta* **1997**, in press.
- (14) Shepherd, R. E.; Chen, Y.; Zhang, S.; Kortes, R. A. Ru(II)–Polyaminopolycarboxylate Complexes for Improved DNA Probes. In *Electron-Transfer Reactions, Advances in Chemistry Series 253*; Isied, S., Ed.; American Chemical Society: Washington, DC, 1997; Chapter 22, pp 367–398.
- (15) Shepherd, R. E.; Zhang, S. *Transition Met. Chem.* **1994**, *19*, 146.
- (16) (a) Chen, Y.; Lin, F.-T.; Shepherd, R. E. *Inorg. Chem.* **1997**, *36*, 818. (b) Chen, Y.; Lin, F.-T.; Shepherd, R. E. *Inorg. Chem. Acta* **1998**, *268*, 287.

plexes are as shown:



Pyrazine's poorer σ donation than pyrimidine, illustrated by free ligand pK_a 's of 0.60 vs 1.31,¹⁵ contributes to poorer to N-1 coordination stability and suggests that η^2 coordination of pyrazines is a possibility.

In this report we examine the ¹H and ¹³C NMR spectra of the pyrazine complex of $[\text{Ru}^{\text{II}}(\text{hedta})]^-$. The $[\text{Ru}^{\text{II}}(\text{hedta})(\text{pz})]^-$ complex has proven unusual in two ways: (1) Unlike $[(\text{NH}_3)_5\text{Ru}(\text{pz})]^{2+}$, at least one isomer of $[\text{Ru}(\text{hedta})(\text{pz})]^-$ complex has fluxional N-1 to N-4 migration at room temperature, and (2) its protonated complex does not undergo a simple lone pair protonation at the N-4 site as has been assumed for other Ru^{II} pyrazines, but rather protonation induces a migration to the two feasible η^2 arrangements as shown pictorially here, in addition to forming the terminally protonated complex:



Experimental Section

Reagents. Pyrazine was 99% gold label quality from Aldrich. $[\text{Ru}(\text{NH}_3)_5\text{Cl}] \text{Cl}_2$ was obtained from Aldrich. $\text{Na}[\text{Ru}(\text{hedta})(\text{H}_2\text{O})] \cdot 4\text{H}_2\text{O}$ was prepared previously^{11–15} and used from those supplies. Equivalent results were obtained using $\text{K}[\text{Ru}(\text{hedta})\text{Cl}]$.²⁵ Weighed amounts of the starting complex were sealed with equivalent or controlled molar ratio amounts of pyrazines in Ar-purged 10 mL glass round-bottom flasks containing Zn/Hg chips and a rice-sized Teflon-coated stirring bar. Each flask was sealed with a rubber septum. Ar-purged D₂O or H₂O as required for an experiment was added via syringe. Zn/Hg was present to reduce traces of Ru^{III} that would interfere with NMR

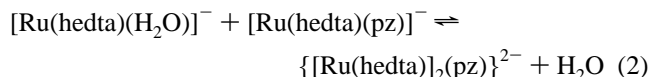
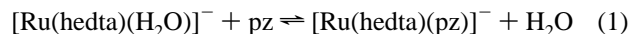
spectroscopy. Syringe techniques and transfers were utilized in filling Ar-purged NMR tubes. To ensure total coordination of the free ligand, a 5% excess of $[\text{Ru}^{\text{II}}(\text{hedta})(\text{H}_2\text{O})]^-$ was maintained with $[\text{Ru}^{\text{II}}]:[\text{pz}]$ ratios of 1.05:1.00. In the case of the binuclear complex the $[\text{Ru}^{\text{II}}]:[\text{pz}]$ ratio was 2.00:1.00, 3.50:1.00, or 5.00:1.00 as needed. The samples for NMR were prepared in D₂O acidified initially with DCl to pD ~ 3.0. The pH/pD rises by exposure of the acidic solution to Zn/Hg and after several hours will reach a final pD of about 6.0. Samples prepared for electrochemical study were either prepared at 2.61×10^{-4} M, 10-fold lower than samples for ¹H NMR, or by transfer and dilution of samples used in NMR experiments, 2.61×10^{-3} M for ¹H NMR and 2.61×10^{-2} M for ¹³C NMR.

Instrumentation. ¹H and ¹³C NMR spectra were recorded on AC300 Bruker NMR spectrometers at 25 °C for samples prepared in D₂O and at -37 °C in D₂O/CD₃OD (50:50 v/v %). For ¹H NMR a DSS reference (0.00 ppm) was added with the D₂O. ¹³C NMR spectra were referenced against 1,4-dioxane at 69.1 ppm. Standard decoupling procedures and integrations were applied to assign ¹H–¹H couplings between ring protons. Calibrations of chemical shifts were also checked by examining the ¹H NMR and ¹³C NMR spectra of free pyrazine, which has singlets at 8.64 ppm for ¹H NMR and 147.26 for ¹³C NMR. These resonances were also used to ensure the absence of free ligand in the product solution or, by doping the sample with excess pyrazine, to show the absence of ligand exchange between bound and free pyrazine.

Electrochemical studies were performed under Ar or N₂ in 0.100 M NaCl as the electrolyte at 22 °C. Measurements were made on an IBM 225 electrochemical analyzer for cyclic voltammetry and differential pulse voltammetry. The standard three-electrode configuration was utilized with a working glassy carbon electrode, a Pt wire auxiliary electrode, and a sodium chloride saturated calomel as the reference. The sweep rates were 50 mV/s for CV and 40 mV/s for DPP, the latter with a 50 mV stepping pulse. The voltage axis was calibrated using the Ru^{III} wave of $[\text{Ru}(\text{bpy})_3](\text{ClO}_4)_2$ at 1.33 V and $[\text{Ru}^{\text{II}}(\text{hedta})(\text{H}_2\text{O})]^-$ at 0.05 V.²⁶ UV–visible spectra were recorded on solutions in 1.00 cm Ar-purged quartz cells, sealed with small rubber septa. Solutions were added via syringe with a syringe needle gas exit. Spectra were recorded on a Varian-Cary 118C spectrophotometer from 750 to 350 nm. pH measurements under Ar were performed using a combination pH probe (calibrated with commercial buffers) inserted through a rubber septum into a bubbler flask attached to an Ar gas line of all glass construction.

Results and Discussions

Electronic Spectral and Electrochemical Changes. Upon the mixing of $[\text{Ru}(\text{hedta})(\text{H}_2\text{O})]^-$ with 1 equiv of pyrazine, a reddish-brown wine colored solution is obtained with an MLCT band maximum at 465 nm ($\epsilon = 6.26 \times 10^3 \text{ M}^{-1} \text{ cm}^{-1}$). This maximum shifts to 533 nm ($\epsilon = 4.70 \times 10^3 \text{ M}^{-1} \text{ cm}^{-1}$) upon acidification to pH ~ 1.90 with 1.0 M Ar-purged HCl. When pyrazine is mixed with $[\text{Ru}^{\text{II}}(\text{hedta})(\text{H}_2\text{O})]^-$, the products are a sensitive function of the mixing conditions. $[\text{Ru}(\text{hedta})(\text{pz})]^-$ with its MLCT maximum at 465 nm forms competitively with binuclear formation (eqs 1 and 2). The binuclear species absorbs



at 533 nm. Binuclear complex formation may be forced to completion by adding excess $[\text{Ru}(\text{hedta})(\text{H}_2\text{O})]^-$. An ϵ at 533 nm of $1.82 \times 10^4 \text{ M}^{-1} \text{ cm}^{-1}$ was determined from samples at

- (17) (a) Matsubara, T.; Creutz, C. *Inorg. Chem.* **1979**, *19*, 1956. (b) Matsubara, T.; Creutz, C. *J. Am. Chem. Soc.* **1978**, *100*, 6255.
 (18) Diamantis, A. A.; Dubrawski, J. V. *Inorg. Chem.* **1981**, *20*, 1142.
 (19) Diamantis, A. A.; Dubrawski, J. V. *Inorg. Chem.* **1983**, *22*, 1934.
 (20) Chatterjee, D.; Bajaj, H. C.; Das, A. *J. Chem. Soc., Dalton Trans.* **1995**, 2497.
 (21) (a) Johnson, C. R.; Chen, Y.; Shepherd, R. E. *Inorg. Chim. Acta* **1998**, *267*, 11. (b) Johnson, C. R. Ph.D. Thesis, University of Pittsburgh, 1982.
 (22) Zhang, S.; Shepherd, R. E. *Transition Met. Chem.* **1992**, *17*, 97.
 (23) Lavallo, D. K.; Fleischer, E. B. *J. Am. Chem. Soc.* **1974**, *94*, 2583.
 (24) (a) Hodges, M. L.; Moody, M. W.; Harman, W. D. *J. Am. Chem. Soc.* **1994**, *116*, 7931. (b) Kopach, M. E.; Harman, W. D. *J. Am. Chem. Soc.* **1994**, *116*, 6581. (c) Hodges, L. M.; Koontz, J. I.; Gonzales, J.; Myers, W. H.; Harman, W. D. *J. Org. Chem.* **1993**, *58*, 4788. (d) Gonzales, J.; Sabat, M.; Harman, W. D. *J. Am. Chem. Soc.* **1993**, *115*, 8857.
 (25) Bajaj, H. C.; van Eldik, R. *Inorg. Chem.* **1989**, *28*, 1980.

- (26) (a) Elliott, M. G.; Zhang, S.; Shepherd, R. E. *Inorg. Chem.* **1989**, *28*, 3036. (b) Zhang, S.; Holl, L. A.; Shepherd, R. E. *Transition Met. Chem.* **1992**, *17*, 390. (c) Zhang, S.; Shepherd, R. E. *Inorg. Chem.* **1988**, *27*, 4712.

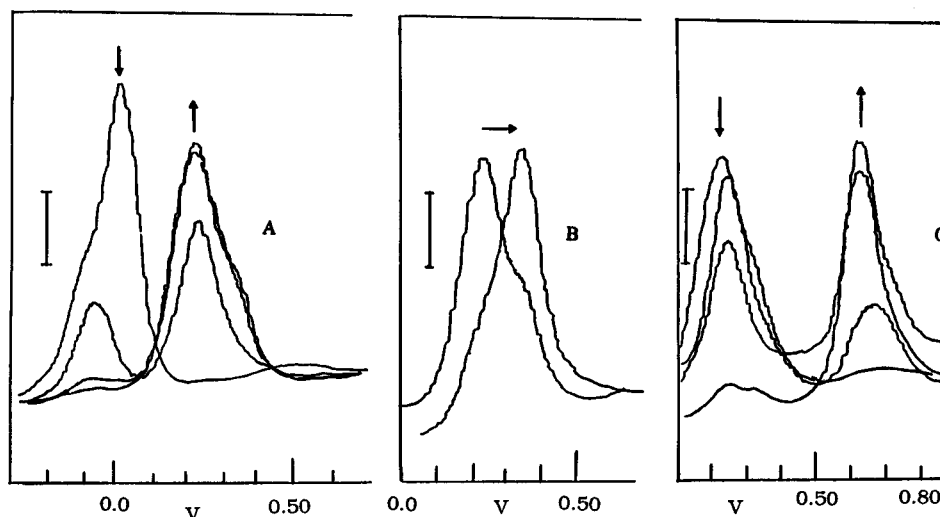
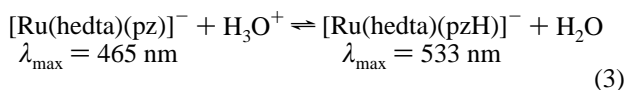


Figure 1. Differential pulse voltammograms of the $[\text{Ru}^{\text{II}}(\text{hedta})]/\text{pyrazine}$ system: (A) $[\text{Ru}(\text{hedta})(\text{H}_2\text{O})]^- = 2.61 \times 10^{-3}$ M in 0.10 M NaCl, 22 °C, $[\text{pz}] = 2.61 \times 10^{-3}$ M (a) before mixing, (b) 2.0 min after mixing, (c) 1 h after mixing, and (d) 4 h after mixing, (B) $[\text{Ru}(\text{hedta})(\text{pz})]^-_{\text{tot}} = 2.61 \times 10^{-3}$ M, $\text{pH}_i \approx 5.0$, $\text{pH}_{\text{final}} = 1.39$ (C); $[\text{Ru}(\text{hedta})(\text{pz})]^-_{\text{tot}} = 2.61 \times 10^{-3}$ M, $\text{pH}_i \approx 6.0$, then adding $[\text{pz}] = 2.35 \times 10^{-2}$ M. Curves are at 0 (mixing), 1.0, 5.0, and 20.0 h. Current markers represent $20 \mu\text{A}/\text{div}$; voltage corrected to NHE.

5.00:1.00 $\text{Ru}^{\text{II}}/\text{pz}$. Different amounts of the binuclear species are produced depending on the method of mixing as shown in Figures S1A and S1B (Supporting Information). Two experiments performed such that the $[\text{Ru}(\text{hedta})(\text{H}_2\text{O})]^-_{\text{tot}}$ and $[\text{pz}]_{\text{tot}}$ concentrations were 1.31×10^{-3} M are presented. In Figure S1A enough solid pz to reach the final total concentration was added directly to a 1.31×10^{-3} M solution of $[\text{Ru}(\text{hedta})(\text{H}_2\text{O})]^-$ over Zn/Hg, while being mixed by an Ar stream passing through the sample. Under these conditions the distribution of mono pz complex to binuclear is 58:42. When solutions are mixed by slowly combining equal volumes of $[\text{Ru}(\text{hedta})(\text{H}_2\text{O})]^-$ and $[\text{pz}]$, each at 2.62×10^{-3} M over Zn/Hg, the amount of the binuclear species is decreased (Figure S1B) such that the distribution of mono to binuclear is 79.1:20.9. The amounts were determined on the basis of the known ϵ of the binuclear ion at 533 nm and curve deconvolution.

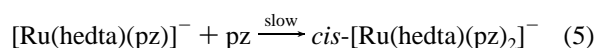
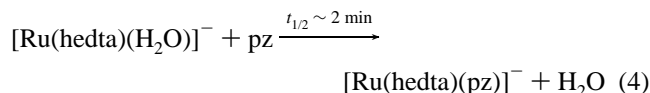
When the pH of the solution is changed, the mono complex undergoes the protonation equilibrium (3) while the binuclear



species is unaffected. This gives rise to the spectral changes as a function of pH shown in Figures S1A and S1B (Supporting Information). Since the protonated species has its MLCT band maximum at 533 nm, which coincides with the MLCT maximum of the binuclear complex, the best data for determination of the $\text{p}K_a$ for $[\text{Ru}(\text{hedta})(\text{pzH})]^-$ were from Figure S1B. The value of 3.1 ± 0.1 was obtained from the 465 nm band. This value compares well with the $\text{p}K_a = 3.45$ determined previously for the 2-methylpyrazine analogue complex, $[\text{Ru}(\text{hedta})(2\text{-CH}_3\text{-pzH})]^-$.⁹ The methyl group should increase the $\text{p}K_a$ relative to pyrazine by an amount less than 1.0 log units on the basis of prior results with the $(\text{NH}_3)_5\text{RuL}^{2+}$ complexes.⁸ Hence the $\text{p}K_a$ of 3.1 ± 0.1 is in good agreement with the anticipated value. Spectra had to be taken immediately after adjustment in the acidic region because a proton-induced further reaction occurs as described later by ^1H NMR but which is detectable by slower changes (Figure S1B) in the visible.

Differential pulse voltammetry was used to show that at 1:1 $[\text{Ru}^{\text{II}}]:[\text{pz}]$, under conditions of $\leq 22\%$ binuclear species, the

mono adduct $[\text{Ru}^{\text{II}}(\text{hedta})(\text{pz})]^-$ is formed at pH = 5.0 (Figure 1). A wave for the $\text{Ru}^{\text{II/III}}$ oxidation appears at ca. 0.20 V vs NHE (Figure 1A), an $E_{1/2}$ value comparable to the monoadducts $[\text{Ru}(\text{hedta})\text{L}]^-$ of other nitrogen base ligands: 0.13 V for pyridine;⁹ 0.12 V for 4-methylpyridine; 0.14 V for pyrimidine.^{14,16} The overlapped binuclear species wave is such that it will not affect the assignment for the mono species. Adjustment to pH 1.39 causes an immediate shift in the wave to 0.35 V vs NHE for the complete conversion of the mono species to the protonated form, pzH^+ , with enhanced π -acceptor properties, is more stabilizing of Ru^{II} causing the positive shift in $E_{1/2}$. An additional change at pH 6.0 occurs over 20 h when the $[\text{Ru}^{\text{II}}]:[\text{pz}]$ ratio is 1:10. A new wave appears at 0.63 V with the loss of the 0.22 V wave (Figure 1C). This process is consistent with the formation of bis complexes, as reported by others for $[\text{Ru}(\text{edta})(\text{H}_2\text{O})]^{2-}$,^{18–20} in two steps:

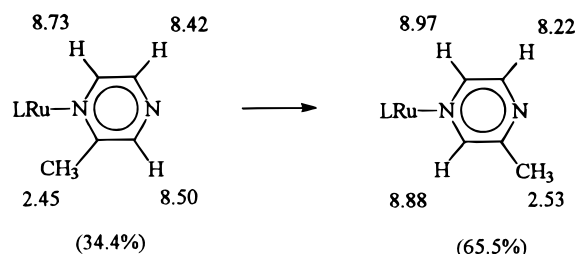


From the half-time of 80 s under second-order equal concentration conditions, a rate constant of $4.8 \text{ M}^{-1} \text{ s}^{-1}$ at 22 °C maybe calculated for the first substitution reaction, comparable to the $15\text{--}32 \text{ M}^{-1} \text{ s}^{-1}$ values reported by Creutz et al. with $[\text{Ru}(\text{edta})(\text{H}_2\text{O})]^{2-}$ and various neutral molecules.¹⁸ The slower second step requires rupture of an in-plane carboxylate– Ru^{II} bond as the limiting step. An estimate of $k_d = 9.6 \times 10^{-5} \text{ s}^{-1}$ is obtained for this process, based on the 2.0 h half-life indicated by Figure 1C. This is in good agreement with the value of $1.57 \times 10^{-4} \text{ s}^{-1}$ for the same process when pyrimidine is the substituting ligand.^{16b}

For comparison, if 2-methylpyrazine is utilized instead of pyrazine, the visible spectral maximum appears at 450 nm ($\epsilon = 1.24 \times 10^4 \text{ M}^{-1} \text{ cm}^{-1}$) at pH 6, changing to a maximum of 525 nm at pH 1.74 ($\epsilon = 1.03 \times 10^4 \text{ M}^{-1} \text{ cm}^{-1}$). The $E_{1/2}$ value for the $\text{Ru}^{\text{II/III}}$ wave is observed at 0.25V vs NHE (pH 6.70), shifting to 0.40V vs NHE (pH 2.32). Rates of substitution are nearly the same for 2- CH_3pz as for pz at equivalent concentration conditions. No time-dependent changes in the visible

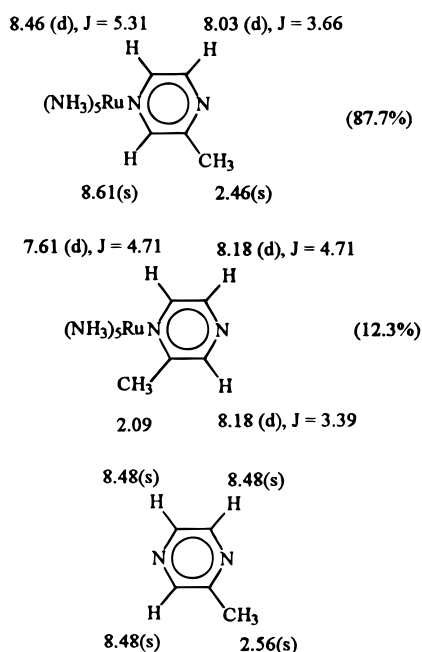
spectra occur after protonation in contrast to the observations with $[\text{Ru}(\text{hedta})(\text{pzH})]^-$.

^1H NMR Observations for 2- CH_3pz Complexes. When $[\text{Ru}(\text{hedta})(\text{D}_2\text{O})]^-$ reacts with 2- CH_3pz at 1:1 ratio (2.61×10^{-3} M), two species are detectable within 30 min after mixing which are readily assigned to "remote methyl" N-4 bound isomer and "adjacent methyl" N-1 bound isomer. The remote N-4 isomer is greater in abundance (65.5%) as would be anticipated for the less sterically hindered addition at N-4. The attachment of anionic Ru^{II} (polyaminopolycarboxylate) complexes to N-heterocyclic rings normally cause downfield shifts for protons α to the site of attachment, upfield shifts for β protons, and smaller upfield shifts at γ positions.²¹ Using these patterns to guide the interpretation of ^1H NMR shifts, we arrived at the following assignments, assisted by peak intensities from integrations (shifts are in ppm):



The hindered isomer decreased with time, slowly converting to the remote isomer.

A confirmation of the two types of N-bound isomers yielding but one observable electrochemical wave was obtained by the separate preparation of two isomers of $[(\text{NH}_3)_5\text{Ru}(2\text{-CH}_3\text{pz})]^{2+}$ by addition of 2- CH_3pz to $[(\text{NH}_3)_5\text{RuOH}_2]^{2+}$ obtained by Zn/Hg reduction of $[(\text{NH}_3)_5\text{RuCl}]\text{Cl}_2$ in water (or D_2O). Only one electrochemical wave is obtained from the product at 0.49 V vs NHE. However, the remote and adjacent isomers were clearly identifiable by ^1H NMR, yielding the following assignments, which are based on the prior observation that cationic metal centers promote upfield shifts of α protons, and downfield shifts for β protons as discussed elsewhere:²¹



The initial substitution reaction is slightly less discriminating

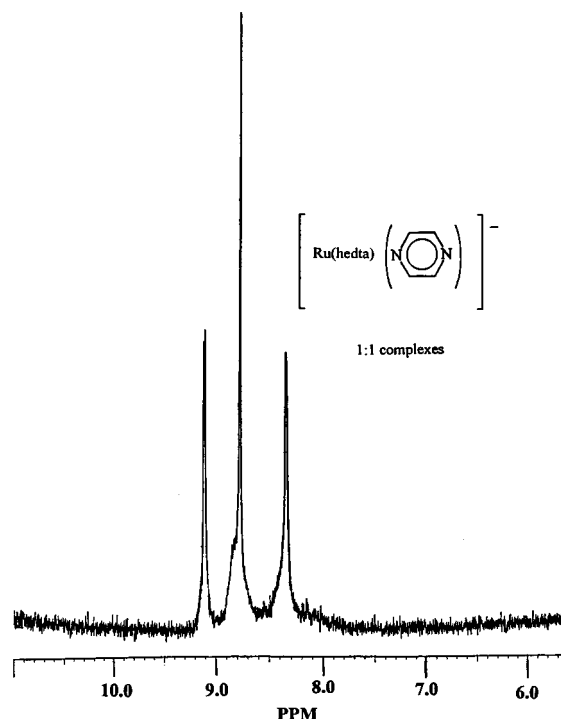


Figure 2. ^1H NMR spectrum of the initial products of $[\text{Ru}(\text{hedta})(\text{D}_2\text{O})]^-$ and pyrazine at 1:1 ratio in D_2O ($T = 22^\circ\text{C}$; $[\text{Ru}^{\text{II}}]_{\text{tot}} = [\text{pz}] = 2.61 \times 10^{-3}$ M; scale in ppm).

for $[\text{Ru}^{\text{II}}(\text{hedta})]^-$ than for $[\text{Ru}^{\text{II}}(\text{NH}_3)_5]^{2+}$. The $[(\text{NH}_3)_5\text{Ru}(2\text{-CH}_3\text{pz})]^{2+}$ complexes are stable and stereochemically rigid on the time scale of the interconversion of adjacent to remote $[\text{Ru}(\text{hedta})(2\text{-CH}_3\text{pz})]^-$ complexes. Therefore, kinetic rearrangement barriers are lower with the Ru^{II} polyaminopolycarboxylate complex.

In the absence of excess ligand, no further changes other than the linkage isomerism which forms 100% remote isomers were observed for the $[\text{Ru}(\text{hedta})(2\text{-Mepz})]^-$ complex in the ^1H NMR spectrum. The identification of distinctly different H2, H3 and H5 2- CH_3pz protons upon coordination is consistent with nonfluxional N-1- or N-4-bound ligand for both pentaammine and hedta^{3-} complexes which stereochemically differentiates all ring positions in both remote and adjacent isomers. The shift patterns follow the known trends for ^1H shifts: 2 protons of $[(\text{NH}_3)_5\text{Ru}(2\text{-CH}_3\text{pz})]^{2+}$ are upfield of the free ligand whereas those of $[\text{Ru}(\text{hedta})(2\text{-CH}_3\text{pz})]^-$ appear downfield for 2 protons in the more stable remote isomers. Addition of excess 2- CH_3pz showed that neither the remote or adjacent isomer of $[\text{Ru}(\text{hedta})(2\text{-CH}_3\text{pz})]^-$ enters into rapid chemical exchange with the free ligand pool as evidenced by an absence of ^1H NMR line broadening or shifting to weighted average ^1H NMR chemical shift positions initially. Upon longer exposure the substitution forming bis complexes occurs.

Pyrazine Complexes. The coordination of pyrazine appears to be kinetically normal initially as evidenced by UV-visible or electrochemical data under neutral pH conditions. However, the ^1H NMR exhibits a different behavior compared to 2- CH_3pz . Adding pyrazine in D_2O to $[\text{Ru}(\text{hedta})(\text{D}_2\text{O})]^-$ inside an NMR tube afforded the spectrum in Figure 2 within 30 min after mixing. Two types of signals are observed in the first 30 min, one 56.2% abundant for two wing peaks and the other 43.8% for the central singlet. Parallel electrochemical studies show the presence of less than 22% of the binuclear species which fortuitously has its ^1H NMR coincident with the central singlet. Hence $\geq 21.8\%$ of the total $(\text{Ru}^{\text{II}}\text{pz})$ monomer species

overlap the binuclear resonance. In a separate experiment, an additional pulse of added pyrazine revealed the free ligand resonance at 8.64 ppm as separate and distinct from both the tall singlet at 8.76 ppm (43.8%) and the 56.2% species with differentiated α and β protons of pyrazine at 9.09 and 8.33 ppm, respectively. Therefore free ligand pyrazine does not enter into ligand exchange for either the major or minor products. Spectra taken over 24 h reveal that the more abundant species by integration converts to the species with the 8.76 ppm singlet. Separate experiments with the stable bis complexes formed at 2.0:1.0 ligand ratio over much longer times show the bis complex has four resonances at 8.65, 8.55, 7.99, and 7.89 ppm that do not match either the initial or final species in Figure 2. The bis complex is also electrochemically different with a characteristic $E_{1/2}$ value of 0.63 V.

It is known that $[\text{Ru}(\text{hedta})(\text{H}_2\text{O})]^-$ exists as a mixture of interconverting stereochemical isomers. The distribution of these is a cis-equatorial (44.1%), trans-equatorial (38.6%), and cis-polar (17.4%) as determined by trapping with methyl vinyl ketone.¹² It can be easily shown that the cis-polar form has a ΔG_f of +0.92 kcal/mol greater than cis-equatorial plus trans-equatorial more open isomers. If ligand addition occurs slowly as for CO and bonding is strong, only one isomer is found in the product due to a shift toward the most stable cis-equatorial form. This is shown by the ^{13}C NMR spectrum of $[\text{Ru}(\text{hedta})\text{CO}]^-$ which has only three types of coordinated carboxylate carbons at 187.76, 186.04, and 184.91 ppm and the anticipated seven unique carbons of the remainder of the hedta^{3-} ligand, required for one isomer (at 71.56, 68.68, 66.93, 65.70, 63.40, 61.10, and 59.62 ppm; Supporting Information Figure 2A). When bonding is weak it should be possible to favor the energetically uphill isomer as long as the process is entropy driven ($\Delta S > 0$). Since the time to obtain the initial ^1H NMR spectrum after 30 min includes time for partial rearrangement, the initial amount of the species calculation based on a first-order decay places the initial amount of the equivalent wing peaks at $\geq 78\%$ of the total Ru^{II} species present. The distribution observed with pyrazine at ca. 30 min trapping is closer to the amount of cis-polar isomer for the fluxional species and cis-equatorial plus trans-equatorial for the initial amount of the rigid isomer(s) with separate α and β ^1H resonances. If these latter isomers convert with time to the cis-polar isomer, the change to a single fluxional species with time is explained. The N-1 to N-4 tumbling motion required for the fluxional molecule will be most assisted by the bumping with the coordinate arms of hedta^{3-} or by forcing a slightly longer Ru–pz bond as anticipated for the cis-polar isomer. The cis-equatorial and trans-equatorial isomers are very open as shown by models, whereas cis-polar is crowded forcing weaker bonding for the cis-polar form. The 1,4-metallotropic shift which accounts for the equivalency of the α and β protons in the fluxional isomer requires a weakly π -bonded intermediate to assist the 1,4-shift. If the tumbling pyrazine is viewed as a ligand with much reduced entropy of translation and rotation compared to a free pyrazine in solution whereas a pyrazine bound in a nonfluxional means at N-1 is a highly ordered pyrazine, one can estimate the ΔS to change from a nonfluxional isomer to that of a fluxional isomer to be approximately of +20 eu (about half the value of a freely translating small molecule). The ΔG for making the more loosely bound fluxional isomer is then favored at 25 °C and is ca. $\Delta G = -6.0$ kcal/mol. Since the ^1H NMR spectra with time shows the fluxional product to be $\geq 98\%$ of the monomeric species and steric factors to achieve the cis-polar arrangement cost 0.92 kcal/mol, any ΔH of $\leq +2.0$ kcal/

mol in converting from cis-equatorial or trans-equatorial isomers to the cis-polar isomer is consistent with the observed product distribution. Since bonding to pyrazine (ΔH_f) is very unlikely to differ by more than 2 kcal/mol among the three possible isomers, it becomes favorable for a shift to the slightly more sterically hindered cis-polar isomer for any ligand if the Ru(II)–ligand bond is not very strong and if the ligand affords fluxional binding sites. Both of these criteria are met for pyrazine which is a poor π -donating ligand and which affords the option of η^2 or N-4 binding modes. Ligands with stronger π -donation should disfavor fluxionality, and indeed, the stronger π -donor pyridazine complex is not fluxional.²⁷ Further discussion of this is taken up after considering the influence of protonation on the coordination of pyrazine to $[\text{Ru}^{\text{II}}(\text{hedta})]^-$. Models also reveal that the pyrazine ring is less exposed to solvation in the cis-polar form which also favors the cis-polar form by releasing solvent and making ΔS even more positive.

To more fully characterize the species responsible for the 8.76 ppm singlet, we obtained the ^1H NMR of the bridged binuclear $\{[\text{Ru}(\text{hedta})_2\text{pz}]^{2-}$ complex, prepared at 2.5:1.0 $[\text{Ru}^{\text{II}}(\text{hedta})(\text{H}_2\text{O})]:[\text{pz}]$. The bridged complex has a signature electrochemical spectrum with two waves at 0.18 and 0.33 V,²² unlike the sole 0.20 V wave of the 1:1 complex. The bridged binuclear species has only α protons on pyrazine next to Ru^{II} centers by symmetry of the molecules. The binuclear complex has a ^1H NMR singlet at 8.76 ppm, fortuitously same as the 1:1 fluxional complex, but the spectrum was obtained purposefully with $[\text{Ru}(\text{hedta})(\text{H}_2\text{O})]^-$ in excess to suppress any dissociation of the binuclear ion. Furthermore, the electrochemical double wave feature and the excess aqua complex were detected for the sample by a DPP spectrum *on the sample taken directly from the NMR tube which produced the 8.76 ppm singlet*. The DPP spectrum of the fully formed binuclear complex and excess $[\text{Ru}(\text{hedta})(\text{H}_2\text{O})]^-$ is shown in Figure 3A. (The uncoordinated excess appears as $[\text{Ru}(\text{hedta})\text{Cl}]$ at -0.11 V.) Whereas the sample at 1:1 $[\text{Ru}(\text{hedta})]^-:[\text{pz}]$ which exhibited the decaying spectrum of Figure 2, and which ultimately also showed an 8.76 ppm singlet, attributed by us to fluxional species, gave an entirely different DPP spectrum (Figure 3B) with waves only at 0.20 V and a smaller component of the bis species at 0.63 V. There was no evidence of the waves at 0.18 and 0.33 V as a pair that is necessary for any binuclear formation accounting for conversion to a single line at 8.76 ppm (Figure 2). The DPP data were collected after 7.0 h of decay for the same sample used in Figure 2, *transferred directly* from the NMR tube. Therefore, a reviewer's suggestions that the decay of the two-line component of the ^1H NMR spectrum to the singlet at 8.76 ppm as representing solely a shift from mono- to binuclear species is invalidated. Furthermore, the absence of any detectable free pz ligand that would need to be released if the final 8.76 ppm were the binuclear species of Figure 2 also rules out binuclear formation as an explanation. Indeed, the fluxional species decays very slowly to substituted bis- $[\text{Ru}(\text{hedta})(\text{pz})_2]^-$ and not the binuclear ion. A DPP spectrum obtained in $\text{D}_2\text{O}/0.1$ M NaCl (not shown) gave results identical to those of Figure 1B for the 1:1 complex as a function of time. This indicates that for the final 1:1 complex adjacent CH positions to N-1 or N-4 binding sites experience the presence of a Ru^{II} center as if both N-1 and N-4 were bound to Ru^{II} but in a species different from the binuclear complex. By contrast, the $[(\text{NH}_3)_5\text{Rupz}]^{2+}$ complex is not fluxional and exhibits separate α and β resonances at 8.13 upfield of free pyrazine and 8.67 downfield

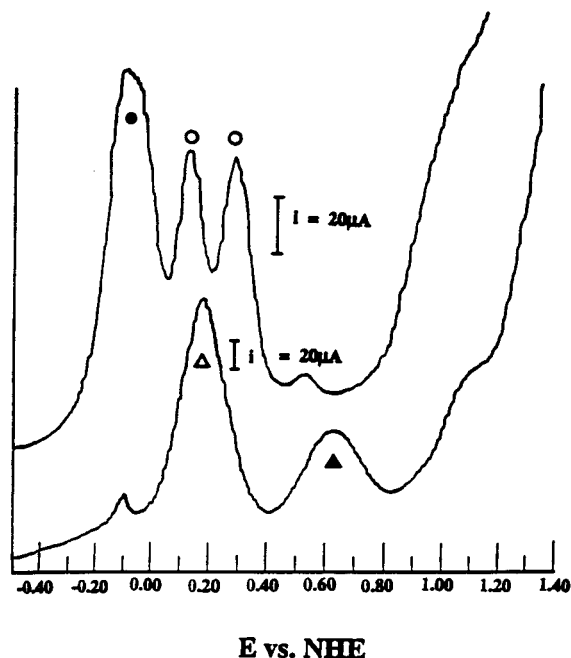


Figure 3. DPP voltammogram of $[\text{Ru}^{\text{II}}(\text{hedta})]$ pyrazine complexes exhibiting a 8.76 ppm singlet: (A) (top curve) $[\text{Ru}^{\text{II}}(\text{hedta})^-]_2[\text{pz}] = 5.00:1.00$ forming $\{[\text{Ru}(\text{hedta})_2(\text{pz})]^{2-}\}^{2-}$ indicated by \circ and 3-fold excess of $[\text{Ru}^{\text{II}}(\text{hedta})(\text{H}_2\text{O})]^-/[\text{Ru}(\text{hedta})\text{Cl}]^{2-}$ indicated by \bullet , spectrum taken at 24.0 h after ^1H NMR showing the 8.76 singlet; (B) (bottom curve) $[\text{Ru}(\text{hedta})^-]_2[\text{pz}] = 1.00:1.00$, reaction time of 7.0 h showing an 8.76 ppm singlet indicated by \triangle and traces of the bis complex (bis complex indicated by \blacktriangle).

of free pyrazine.²³ This is the correct order of shifts for cationic metal centers acting on N-heterocyclic rings, which is the reverse of anionic metal sites,²¹ as shown herein.

The ^{13}C NMR spectra were obtained for free pyrazine, the single fluxional $[\text{Ru}(\text{hedta})(\text{pz})]^-$ product obtained in 1 day with the 8.76 ppm ^1H NMR singlet, and of the $\{[\text{Ru}(\text{hedta})_2(\text{pz})]^{2-}\}^{2-}$ binuclear complex synthesized at 2:1 $[\text{Ru}^{\text{II}}]:[\text{pz}]$ ratio. The free ligand pyrazine carbons resonate at 147.76 ppm, whereas the fluxional complex appears at 152.44 ppm (Figure S2B of the Supporting Information) and the binuclear complex at 152.40 ppm. Again, the metalation causes downfield shifts from the free ligand value. However, the 1:1 $[\text{Ru}(\text{hedta})(\text{pz})]^-$ complex, observed after 1 day to allow for complete stereochemical rearrangement, exhibits the same ^{13}C shift for all ring carbons as if having two Ru^{II} centers locked in place adjacent to N-1 and N-4. The ^{13}C NMR spectra of both the 1:1 and the binuclear complexes show that the three carboxylates remain coordinated even after several days. ^{13}C NMR shifts were observed at 189.09, 187.28, and 186.22 ppm for the 1:1 complex and 189.06, 187.27, and 186.22 for the $[\text{Ru}(\text{hedta})]$ carboxylates of the binuclear species. Coordinated carboxylates appear between 184 and 190 ppm, whereas free pendant carboxylates would be seen at ca. 175 to 178 ppm. The latter were absent from both spectra. For the “hedta³⁻” region the 1:1 complex had six distinct resonance signals with two overlapped at 59.22 ppm and others at 70.03, 68.56, 67.24, 66.28, and 63.38 ppm. These were nearly the same in the binuclear complex with resonances at 69.98, 68.48, 67.13, 66.25, 63.33, and 59.19 ppm. There are of 3 carboxylato ^{13}C resonances and 7 ^{13}C resonances that are observed in the “hedta³⁻” region that are observed. This number of ^{13}C signals is only compatible with one stereochemical isomer of the $[\text{Ru}^{\text{II}}(\text{hedta})]^-$ fragment being bound at the N-1 and/or N-4 sites in the final 1:1 and binuclear complexes, respectively.

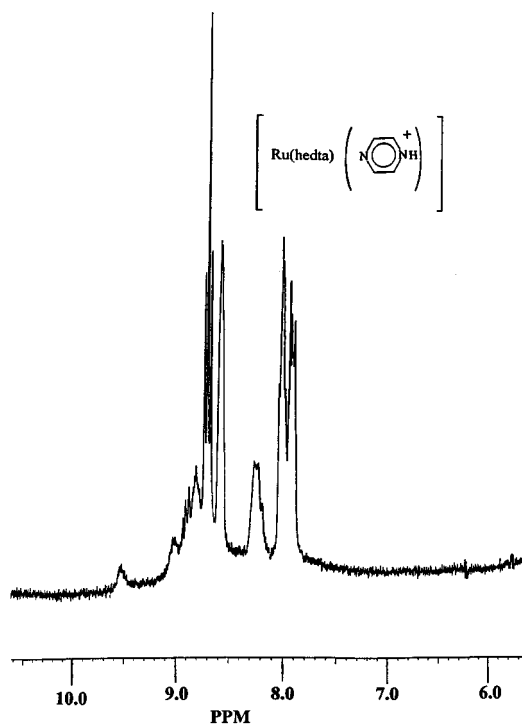
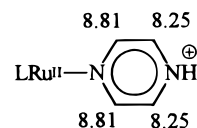


Figure 4. ^1H NMR spectrum of the protonated species formed from $[\text{Ru}(\text{hedta})\text{pz}]^-$ at $\text{pD} \sim 1.5$ in D_2O ($T = 22^\circ\text{C}$; $[\text{Ru}^{\text{II}} \text{ complexes}]_{\text{tot}} = 2.61 \times 10^{-3} \text{ M}$; scale in ppm).

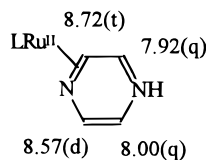
The samples of the mono- and binuclear complexes were rigorously checked after the ^{13}C NMR data accumulation by the DPP method. The species were observed to be 1:1 and 2:1 complexes, by their signature electrochemical wave forms.

Protonation Reaction. An additional proof that the binuclear sample and 1:1 adduct sample were not the same despite seeming equivalence of their ^1H and ^{13}C NMR shifts was obtained by the influence of acidity on the electrochemical DPP waves and the ^1H NMR spectra. The ^1H NMR spectra of the binuclear complex did not change immediately, nor does the two-wave $E_{1/2}(1) = 0.18 \text{ V}$, $E_{1/2}(2) = 0.33 \text{ V}$ pattern change on acidification with DCl or HCl. However, treating the 1:1 complex with DCl to $\text{pD} \sim 1.5$ causes a rapid change in the ^1H NMR spectrum as shown in Figure 4. Decoupling procedures revealed that the four major sets of resonances shown in Figure 4 are interrelated. These multiplets appear at 8.72 (t), 8.57 (d), 8.00 (q), and 7.92 (q). Decoupling shows interaction between the 8.72 and 7.92 ppm multiplets and 8.57 and 8.00 ppm near quartets. A less abundant species with ^1H NMR connectivities appears with near doublets at 8.81 and 8.25 ppm. A smaller set of four appear at 9.51, 9.01, 8.85, and 8.15 ppm. The presence of four distinct proton shifts for the major species (63%) in $[\text{Ru}(\text{hedta})(\text{pzH})]^+$ is not compatible with simple proton addition to the terminal N-4 lone pair, “freezing out” fluxionality that is indicated by ^1H NMR and ^{13}C NMR methods for $[\text{Ru}(\text{hedta})(\text{pz})]^-$ in neutral solution. This would give separate α and β sets. However, the minor species (16.7%) with near doublets is consistent with the anticipated rigid, terminally protonated species with the indicated shift pattern:

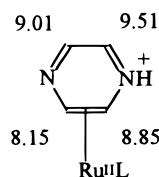


The other two structures shown in the Introduction, e.g. η^2 -

(1,2) and $\eta^2(2,3)$ will account for the remaining patterns given by the ^1H NMR of $[\text{Ru}(\text{hedta})(\text{pzH})]$ species. The $\eta^2(1,2)$ type requires four discrete ^1H resonances. The decoupling procedures implicate connectivities which are consistent with the shift assignment as shown:



Although the shift positions are very similar to the bis complex, the bis complex lacks the distinguishing triplet at 8.72 ppm. Therefore the new species is not the bis complex. Nor do solutions exhibit liberated $[\text{Ru}(\text{hedta})(\text{H}_2\text{O})]^-$, needed to form a bis species, as shown by supporting electrochemical studies. If across-the-ring coupling is strong, splittings similar to doublets-of-doublets are anticipated, with the protons nearer to H^+ upfield of 8.64 ppm, and those nearer to Ru^{II} should be downfield of 8.64. The four resonances are grouped into two pseudo α , β sets: 8.72, 8.57 and 7.92, 8.00 ppm with the 8.57 and 8.00 pair least perturbed by the presence of Ru^{II} and the 8.72 and 7.92 pair more significantly affected. We assign the 8.72 ppm resonance as most near to $[\text{Ru}^{\text{II}}(\text{hedta})]^-$; the 7.91 ppm resonance would be consistent with a proton shifted most upfield, being α to H^+ and β to Ru^{II} . The least abundant species has resonance components at 9.51 and 9.01 and buried contributions at 8.25 and 8.15 that are revealed by integration procedures. We assign these to a small amount of $\eta^2(2,3)$ isomer (20.3%) with the following ^1H shifts:



We have assigned the 8.85 and 8.15 ppm pair to the protons nearest Ru^{II} because of the anticipated upfield shift for $\eta^2(\text{C}=\text{C})$ compounds. However, the amounts of this isomer have precluded thorough study, and arguments could be presented to reverse the tentative assignment shown in the drawing here. The various ^1H and ^{13}C shift data for the major species prior to protonation are presented in Table 1 for reference.

Two issues remain to be explained: (1) why the pyrazinium form binds in the η^2 fashion but the neutral pyrazine ring adopts N-1/N-4 coordination; (2) why 2-methylpyrazine does not adopt η^2 coordination. The inductive influence of methyl groups enhance the σ -donating capacity of the diazines. The amount of η^2 pyrimidine complexes at final equilibrium with N-1 coordination decreases from 98% for pym with no CH_3 groups to 43% for 4- CH_3 pym and 32% for 4,6- Me_2 pym.¹⁶ Therefore methyl σ donation strengthens the $\text{Ru}(\text{II})-\text{N}$ bond, contributing to a higher activation barrier for N-1 to η^2 migrations.¹⁴ Hence the effect for 2- CH_3 pz not adopting η^2 structures upon protonation follows this trend. Conversely, withdrawing groups such as exo carbonyls in the pyrimidine nucleobases favor η^2 coordination, e.g. uridines and uracils.^{9,12} These effects explain the second of the two proposed questions.

The fluxionality of the $[\text{Ru}(\text{hedta})(\text{pz})]^-$ complex shows that the σ bonding from Ru^{II} to pyrazine N-1 must not be strong or that the barrier to the $\text{Ru}^{\text{II}}-\text{pz}$ σ bond rupture is low. Tumbling is rapid on the NMR time scale as shown by the fluxionality at

Table 1. NMR and Electrochemical Data for Pyrazine Complexes

complex	δ (ppm)	
	^1H NMR 300 MHz	^{13}C NMR 125 MHz
	8.64	147.26
$[(\text{NH}_3)_5\text{RuN}(\text{pyrazine})]^{2+}$		
α	8.13 ^a	
β	8.67 ^a	
$[(\text{NH}_3)_5\text{RuN}(\text{pyrazine})\text{NRu}(\text{NH}_3)_5]^{4+}$	8.20 ^a	
$[(\text{hedta})\text{RuN}(\text{pyrazine})]^-$		
fluxional isomer	8.76 ^b	152.44
rigid isomer α	9.09	
β	8.33	
$E_{1/2}$: 0.24 V, pH = 7; 0.35 V, pH \approx 1		
$[(\text{hedta})\text{RuN}(\text{pyrazine})\text{NRu}(\text{hedta})]^{2-}$	8.76	152.40
$E_{1/2} = 0.18$ V; $E_{1/2}(2) = 0.33$ V		
$[(\text{hedta})\text{Ru}(\text{pyrazine})_2]^-$	8.65	
$E_{1/2} = 0.63$ V, pH \approx 7		

^a Lavaile, D. K.; Fleischer, E. B. *J. Am. Chem. Soc.* **1992**, *94*, 2583.
^b Down to -40 °C in $\text{CD}_3\text{OD}/\text{D}_2\text{O}$.

298 K. No evidence of freezing out the fluxionality was observed down to -37 °C in 50% $\text{D}_2\text{O}/\text{CD}_3\text{OD}$ where a singlet at 8.70 ppm is still observed (Supporting Information Figure S3), slightly shifted from the 8.67 ppm value at 22 °C.

Protonation at N-4 further depletes σ electron density at the N-1 donor, making pzH^+ an even poorer donor to $[\text{Ru}^{\text{II}}(\text{hedta})]^-$. Upon protonation, the electronic distribution within the ring becomes polarized toward the NH^+ end of pzH^+ . This σ drain on orbital density improves the π -acceptor ability due to lower electron repulsion and increased charge on carbons at the end near Ru^{II} . The weakened $\text{Ru}^{\text{II}}-\text{N}$ σ bonding is then in competition with the $\eta^2(1,2)$ bonded alternative. With protonation and electronic polarization the net aromaticity and delocalization of the ring decreases. That is, pzH^+ is less delocalized than the neutral pyrazine, again contributing to a lower rearrangement N-1 to η^2 barrier for the pyrazinium system. Once the Ru^{II} center has migrated from the σ lone pair at N-1 onto the π system there should be a pathway which allows migration to the neighboring $\eta^2(2,3)$ position. However, the process is not facile as observed by separate resonances for each species. That the migrations are not fluxional between $\eta^2(1,2)$ and $\eta^2(2,3)$ species is in line with the statistically greater number (2:1 chances) for $\eta^2(1,2)$ compared to $\eta^2(2,3)$ interactions, but more importantly, the electron-withdrawing power of a nitrogen atom is greater than carbon, lending itself to greater ionic resonance energy in the η^2 bonding of Ru^{II} to $\text{N}=\text{C}$ of the $\eta^2(1,2)$ species than to $\text{C}=\text{C}$ of the $\eta^2(2,3)$ species. Last, the influence of protonation which promotes migration of $[\text{Ru}^{\text{II}}(\text{hedta})]^-$ to η^2 positions of the pyrazinium ring has a commonality with behavior we have recently reported with the pyridazine complex of $[\text{Ru}^{\text{II}}(\text{hedta})(\text{pyd})_2]^-$ ($n = 1$ or 2).²⁷ The pyridazine complexes are stereochemically rigid and do not exhibit 1,2-metallotropic shifts up to 60 °C. However, when

the $\text{pD} \leq 1.0$, the $[\text{Ru}^{\text{II}}(\text{hedtaH})(\text{pydH})]^+$ complex exhibits a 1,2-metallotropic shift. Weakened $\text{Ru}^{\text{II}}\text{--pydH}^+$ σ bonding has been attributed to causing this phenomena. Thus, decreased σ donation by an N-heterocyclic base toward the Ru^{II} (polyamino polycarboxylate centers) appear to destabilize the bonding and to favor migrations, either to other η^2 locations on the π -cloud or to another available nitrogen lone pair.

Acknowledgment. We gratefully acknowledge general laboratory support from the Research Corp. and Petroleum Research Fund. We also thank S. Zhang for providing the ^{13}C NMR spectrum of $\text{Na}[\text{Ru}(\text{hedta})\text{CO}]$.

Supporting Information Available: Figure S1A, showing visible spectral changes upon acidification of $[\text{Ru}(\text{hedta})(\text{pz})]^-$ prepared by adding solid pyrazine to $[\text{Ru}(\text{hedta})(\text{H}_2\text{O})]^-$ at 1.31×10^{-4} M, Figure S1B, showing the same as Figure S1A with sample preparation at dilute solution conditions, Figure S2A, showing the ^{13}C NMR spectrum of $[\text{Ru}(\text{hedta})\text{CO}]^-$, Figure S2B, showing the ^{13}C NMR spectrum of the fluxional $[\text{Ru}(\text{hedta})(\text{pz})]^-$ complex, and Figure S3, showing the 236 K ^1H NMR spectrum of the fluxional $[\text{Ru}(\text{hedta})(\text{pz})]^-$ complex in 50% $\text{D}_2\text{O}/50\%$ CD_3OD (5 pages). Ordering information is given on any current masthead page.

IC961269F